PHYSICAL REVIEW VOLUME 135, NUMBER 3A 3 AUGUST 1964

Observation of Magnetoacoustic Geometric Resonances for Magnetic Field at Arbitrary Direction*

Y. ECKSTEIN, J. B. KETTERSON, AND S. G. ECKSTEIN
Argonne National Laboratory, Argonne, Illinois
(Received 25 March 1964)

Oscillations have been observed in the magnetoacoustic attenuation of Sb for sound propagated along the binary axis, and the magnetic field in the binary-bisectrix plane and the binary-trigonal plane. The oscillations were of sinusoidal, rather than of resonant character, even for $q\|H$, and were therefore interpreted as geometric resonances. Expressions are given for the period as a function of angle, and the data were compared with the resulting theoretical curves. Of the eight effective mass parameters necessary to evaluate the theoretical expressions, all seven of the parameters measured in a previous Shubnikov-de Haas experiment were used, and the remaining parameter was taken from the present experiment. The resulting curves are in good agreement with the data. The reciprocal effective mass tensors have been re-evaluated by using the new parameter.

MAGNETOACOUSTIC geometric resonances for the magnetic field perpendicular to the direction of sound propagation are well understood both theoretically and experimentally. However, the interpretation of such oscillations for the parallel field case has not been completely clear. Recently, two different interpretations of such effects have been proposed, by Daniel and Mackinnon[1] and by Quinn.[2] In this paper we report the observation of geometric resonances in the attenuation of sound in antimony, for arbitrary direction of the magnetic field, including the direction parallel to the sound wave. Because of the simple band structure of antimony, namely, ellipsoidal energy surfaces,[3,4] the period of oscillation can be calculated theoretically, for arbitrary field direction, using the results of a previous investigation.[5] For the special case of parallel field, our interpretation agrees with that of Quinn.

A 138-Mc/sec sound wave was propagated in the direction of the binary axis. The magnetic field, which ranged from 0 to 300 G, was rotated in the binary-bisectrix and binary-trigonal planes at regular intervals. The usual pulse-echo technique was used, and oscillations of the echo height were recorded on an x-y recorder, using a boxcar integrator. These oscillations were found to be periodic in $1/H$. (See Fig. 1.) The experimentally observed periods are plotted as a function of magnetic field angle in Fig. 2.

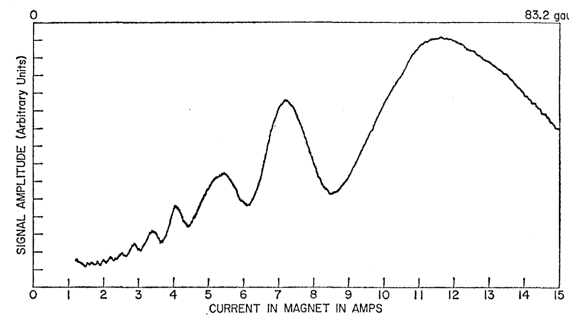

FIG. 1. Experimental curve for $q\|H\|$binary axis for longitudinal sound wave of 138-Mc/sec frequency. Note that the curve is more of sinusoidal than of resonant character. Parallel field effects other than geometric resonances predict spiky behavior.

The parallel field effect may be explained in the same way as the perpendicular field effect geometric resonances. These resonances occur when there is a matching of extremal dimension of the electron orbit in real space with a multiple of the wavelength. For an anisotropic Fermi surface, the plane of orbit of the electrons in real space is not perpendicular to the magnetic field, as it is for a spherical energy surface. Hence, the sound wave vector will have a nonzero projection upon the plane of the orbit, even if the direction of the sound is parallel to the magnetic field.

We calculated the period of oscillation for arbitrary angle between the magnetic field and the sound wave, using Eq. (8) of Ref. 5. This reference discusses the possibility of observation on nonextremal orbits. However, the oscillations due to these nonextremal orbits will not be strictly periodic in $1/H$; and in this experiment, we observed only oscillations which are periodic in $1/H$. Therefore, the orbits which we observed are essentially the extremal orbits, i.e., $(\mathbf{p}\cdot\hat{H})\approx 0$. Setting $\nu=0$ in Eq. (8), one finds the general formula for the period of the extremal orbits:

$$\Delta\left(\frac{1}{H}\right)=\frac{e\lambda}{2c}\frac{1}{(2mE_F)^{1/2}}\times\left[\frac{|\alpha|\,(\hat{H}\cdot\boldsymbol{\alpha}^{-1}\cdot\hat{H})^2}{(\hat{q}\cdot\boldsymbol{\alpha}\cdot\hat{q})(\hat{H}\cdot\boldsymbol{\alpha}^{-1}\cdot\hat{H})-(\hat{q}\cdot\hat{H})^2}\right]^{1/2}, \quad (1)$$

where $\hat{H}$ and $\hat{q}$ are unit vectors in the direction of the magnetic field and the sound wave vector, $\boldsymbol{\alpha}$ is the ellipsoid tensor defined by $2mE_F=\mathbf{p}\cdot\boldsymbol{\alpha}\cdot\mathbf{p}$, and $|\alpha|$ is the determinant of $\boldsymbol{\alpha}$.

* Based on work performed under the auspices of the U. S. Atomic Energy Commission.

[1] M. R. Daniel and L. Mackinnon, Phil. Mag. **8**, 537 (1963).
[2] J. J. Quinn, Phys. Rev. Letters **11**, 316 (1963).
[3] J. B. Ketterson and Y. Eckstein, Phys. Rev. **132**, 1885 (1963).
[4] G. N. Rao, N. H. Zebouni, C. G. Grenier, and J. M. Reynolds, Phys. Rev. **133**, A141 (1964).
[5] S. G. Eckstein, Phys. Rev. Letters **12**, 369 (1964).

The experimental data on antimony to date have been explained by assuming a two-band model, each band being made up of three (or six) tilted ellipsoids. The principal electron ellipsoid is denoted by α and the principal hole ellipsoid by β. In each case $\alpha_{12}=\alpha_{13}=0$ and $\beta_{12}=\beta_{13}=0$. The remaining ellipsoids are derived by rotating the principal ellipsoids around the z axis by $\pm 120°$.

In this experiment, the following geometry was used: $\hat{q}=(1,0,0)$, $\hat{H}=(\cos\theta, \sin\theta, 0)$; and $\hat{q}=(1,0,0)$, $\hat{H}=(\cos\phi, 0, \sin\phi)$. By substitution in Eq. (1), the period for the principal electron ellipsoid for H in the x-y plane is found to be

$$\Delta_1^e\left(\frac{1}{H}\right)=\frac{e\lambda}{2c}\frac{1}{(2mE_F)^{1/2}}(\alpha_{33})^{1/2}\times\left[\sin\theta+\frac{\gamma^e}{\alpha_{11}\alpha_{33}}\left(\frac{1}{\sin\theta}-\sin\theta\right)\right], \quad (2)$$

where $\gamma^e=\alpha_{22}\alpha_{33}-\alpha_{23}^2$. The principal electron ellipsoid period for H in the x-z plane is

$$\Delta_1^e\left(\frac{1}{H}\right)=\frac{e\lambda}{2c}\frac{1}{(2mE_F)^{1/2}}(\alpha_{22})^{1/2}\times\left[\sin\phi+\frac{\gamma^e}{\alpha_{11}\alpha_{22}}\left(\frac{1}{\sin\phi}-\sin\phi\right)\right]. \quad (3)$$

The period for the remaining two electron ellipsoids for H in the x-y plane is given by

$$\Delta_{2,3}^e\left(\frac{1}{H}\right)=\frac{e\lambda}{2c}\frac{1}{(2mE_F)^{1/2}}\times\frac{N^\pm}{[(\alpha_{11}+3\alpha_{22})N^\pm-16\alpha_{11}\gamma^e\cos^2\theta]^{1/2}}, \quad (4)$$

where

$$N^\pm=(\alpha_{11}\alpha_{33}+3\gamma^e)+2(\alpha_{11}\alpha_{33}-\gamma^e)(\cos^2\theta\pm 3^{1/2}\sin\theta\cos\theta).$$

The period of the rotated ellipsoids for H in the x-z plane is given by

$$\Delta_{2,3}^e\left(\frac{1}{H}\right)=\frac{e\lambda}{2c}\frac{1}{(2mE_F)^{1/2}}\times\frac{M^\pm}{[(\alpha_{11}+3\alpha_{22})M^\pm-16\alpha_{11}\gamma^e\cos^2\phi]^{1/2}}, \quad (5)$$

where

$$M^\pm=4\alpha_{11}\alpha_{22}+(3\alpha_{11}\alpha_{33}+\gamma^e-4\alpha_{11}\alpha_{22})\cos^2\phi \pm 4(3)^{1/2}\alpha_{11}\alpha_{23}\sin\phi\cos\phi.$$

The periods for the hole ellipsoids, $\Delta_1^h(1/H)$ and $\Delta_{2,3}^h(1/H)$, are obtained by substituting β for α in Eqs. (2)–(5).

In Shubnikov-de Haas experiments[3,4] the combinations $\alpha_{11}\alpha_{22}$, $\alpha_{11}\alpha_{33}$, and $\alpha_{11}\alpha_{23}$ have been observed for the electron band, and the same combinations of the β_{ij} have been observed for the hole band. On the other hand, only one of the parameters γ was observed directly, and it could not be unambiguously ascribed to either carrier. When this parameter is ascribed to the hole band, as in Refs. 3 and 4, agreement with the present experiment is poor. We therefore ascribed the measured γ value to the electron band, and, as a fourth hole parameter, chose β_{33} as measured by the period at $H\|y$ [cf. Eq. (2) for $\theta=\pi/2$]. The resulting ellipsoid tensors are given by[6]

$$\alpha=\begin{bmatrix}1.011 & 0 & 0\\ 0 & 0.330 & 0.348\\ 0 & 0.348 & 0.557\end{bmatrix}\times 10^{14}E_F \quad (6)$$

and

$$\beta=\begin{bmatrix}0.618 & 0 & 0\\ 0 & 0.0367 & 0.0686\\ 0 & 0.0686 & 1.012\end{bmatrix}\times 10^{14}E_F. \quad (7)$$

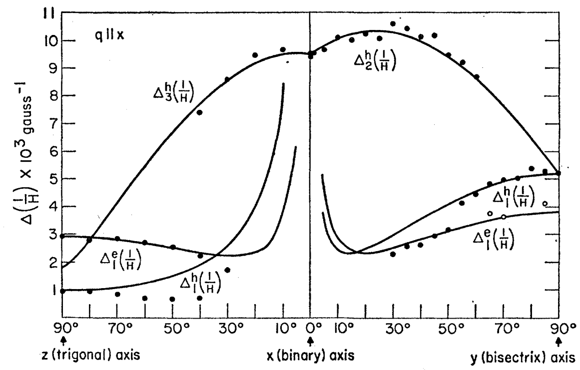

FIG. 2. Periods of oscillation as a function of magnetic field angle. $\Delta_1^e(1/H)$ refers to the principal electron ellipsoid; $\Delta_1^h(1/H)$ to the principal hole ellipsoid; and $\Delta_{2,3}^h(1/H)$ to the rotated hole ellipsoids. The other theoretical curves were omitted because they did not correspond to any experimental data. The open circles are periods derived from beats. The period of the principal ellipsoids is infinite at $\hat{H}\|\hat{q}$ (0°).

The theoretical curves using these parameters are plotted in Fig. 2, and the agreement with the experimental data is quite satisfactory for all branches, except for Δ_1^h in the x-z plane. This discrepancy may be due to another carrier, evidence of which has been seen in Ref. 3, whose period at $H\|z$ accidently coincides with the hole period. The discrepancy might also be due to a nonellipsoidal character of the hole band. The nonellipsoidal character would have its most pronounced effects when H is in the x-z plane[7]; these effects are now under theoretical investigation.

[6] The Shubnikov-de Haas parameters used were those of Ref. 3. They agree with the parameters of Ref. 4 within experimental error. The measured value of β_{33} agrees with the value observed by L. Eriksson, O. Beckman, and S. Hornfeldt (to be published); it does not, however, agree with the value of β_{33} derived in Refs. 3 and 4.

[7] M. H. Cohen, Phys. Rev. **121**, 387 (1961).

Since the experimental data in the neighborhood of $\hat{H}||\hat{q}$ are in satisfactory agreement with the theory given here, there is no experimental evidence of the parallel field effect suggested by Daniel and Mackinnon.

We should like to comment upon the application of this effect to the study of band structure. If the magnetic field is parallel to the sound wave vector, then we measure the linear dimension of the orbit parallel to the magnetic field. However, this gives no *direct* information about the orbit in p space, because, as known, $\mathbf{p}(t)=(e/c)[\mathbf{r}(t)\times\mathbf{H}]$. Thus, that part of the orbit in real space which is parallel to the magnetic field does not contribute to the p-space orbit at all. However, if a model of the Fermi surface is already known, then the equations of motion may be solved to find the orbit in real space, as was done for the ellipsoidal case, and additional information regarding the Fermi surface will be obtained. The parallel field effect might also find application in singling out those sheets of the Fermi surface which are tilted with respect to a symmetry axis. For example, if $\hat{q}||\hat{H}||[001]$ axis of tin, only four of a possible ten sheets predicted by the free electron model of the Fermi surface would contribute to geometric resonances.[8]

[8] A. V. Gold and M. G. Priestley, Phil. Mag. 5, 1089 (1960).

PHYSICAL REVIEW VOLUME 135, NUMBER 3A 3 AUGUST 1964

Infrared Lattice Vibrations in Calcium Tungstate and Calcium Molybdate

A. S. Barker, Jr.
Bell Telephone Laboratories, Murray Hill, New Jersey
(Received 9 March 1964)

The infrared active lattice vibrations of single-crystal $CaWO_4$ and $CaMoO_4$ have been studied by taking polarized reflection spectra in the region 1 to 130 μ. Four infrared phonon modes vibrate with the electric vector E parallel to the c axis and four with E perpendicular to the c axis in each material. A classical oscillator dispersion analysis is carried out to give the mode strengths, frequencies, and linewidths of the eight infrared modes. The frequencies of the eight corresponding longitudinal optic modes are found from the dispersion analysis. A symmetry study of the zero wave vector vibrations is carried out for the Scheelite structure which predicts four infrared modes for $E||c$ axis and four for $E\perp c$ axis as well as 13 Raman modes and 3 inactive modes. A study is made of apparent failure of the classical oscillator model near one of the strong modes.

INTRODUCTION

Large single crystals of calcium tungstate and molybdate have recently become available as a result of perfection of the Czochralski growth method for oxide systems.[1,2] These crystals can be readily doped with rare-earth ions during growth. The doped crystals are the subject of much current optical maser study.[3,4] This paper describes measurements of the infrared reflectivity for the pure materials. Very little has been done since Coblentz's infrared work on $CaWO_4$ in 1908.[5] In that work one restrahlen band was reported near 12 μ for an unoriented sample. In the present work eight infrared allowed modes are seen in the reflection spectra. A dispersion analysis is carried out which yields the strengths, resonant frequencies, and linewidths of the infrared-active phonon modes and the frequencies of the associated longitudinal optic modes. The results are shown to be in agreement with a study made of the group character table for the Scheelite structure.

[1] K. Nassau and A. M. Broyer, J. Appl. Phys. 33, 3064 (1962).
[2] S. Preziosi, R. R. Soden, and L. G. Van Uitert, J. Appl. Phys. 33, 1893 (1962).
[3] L. F. Johnson, J. Appl. Phys. 34, 897 (1963). L. F. Johnson and R. A. Thomas, Phys. Rev. 131, 2038 (1963).
[4] L. F. Johnson, L. G. Van Uitert, J. J. Rubin, and R. A. Thomas, Phys. Rev. 133, A494 (1964).
[5] W. Coblentz, *Supplementary Investigations of Infrared Spectra* (The Carnegie Institution, Washington, 1908), Publication No. 97, p. 16.

EXPERIMENTAL

Boules of undoped $CaWO_4$ and $CaMoO_4$ were obtained and oriented by x ray. Two slabs about 1 by 1 by 0.4 cm were then cut from each boule. The slabs were cut so that the large face was perpendicular to the c axis in one sample and perpendicular to the a axis in the other. The faces and some edges were then polished. Both materials are quite soft. Satisfactory results were obtained by progressing from 400 grit sandpaper to Buehler M305 abrasive then directly to Linde-A polishing compound using water slurrys on plate glass laps. After polishing the samples, the c axis could be located quite easily from the optic figure seen with crossed polaroids.

Room-temperature polarized reflection spectra were taken for the electric vector E parallel to the c axis and then for E parallel to an a axis. This choice selects the major and minor axes of the dielectric ellipsoid and will thus specify the complete optic behavior when the reflection spectra are suitably analyzed. The measure-